

RESEARCH ARTICLE

Cellular velocity, electrical persistence and sensing in developed and vegetative cells during electrotaxis

Isabella Guido^{1*}, Douglas Diehl¹, Nora Aleida Olszok¹, Eberhard Bodenschatz^{1,2,3}

1 Max-Planck Institute for Dynamics and Self-organization, Göttingen, Germany, **2** Institute for Dynamics of Complex Systems, Georg-August-University Göttingen, Göttingen, Germany, **3** Laboratory of Atomic and Solid-State Physics, Cornell University, Ithaca, NY, United States of America

* isabella.guido@ds.mpg.de



OPEN ACCESS

Citation: Guido I, Diehl D, Olszok NA, Bodenschatz E (2020) Cellular velocity, electrical persistence and sensing in developed and vegetative cells during electrotaxis. PLoS ONE 15(9): e0239379. <https://doi.org/10.1371/journal.pone.0239379>

Editor: Xin Yi, Peking University, CHINA

Received: April 23, 2020

Accepted: September 7, 2020

Published: September 18, 2020

Copyright: © 2020 Guido et al. This is an open access article distributed under the terms of the [Creative Commons Attribution License](https://creativecommons.org/licenses/by/4.0/), which permits unrestricted use, distribution, and reproduction in any medium, provided the original author and source are credited.

Data Availability Statement: All relevant data are within the paper and its Supporting Information files.

Funding: E.B. and I.G. Support from the MaxSynBio Consortium which is jointly funded by the Federal Ministry of Education and Research of Germany and the Max Planck Society. <https://www.maxsynbio.mpg.de/13480/maxsynbio> The funders had no role in study design, data collection and analysis, decision to publish, or preparation of the manuscript.

Competing interests: The authors have declared that no competing interests exist.

Abstract

Cells have the ability to detect electric fields and respond to them with directed migratory movement. Investigations identified genes and proteins that play important roles in defining the migration efficiency. Nevertheless, the sensing and transduction mechanisms underlying directed cell migration are still under discussion. We use *Dictyostelium discoideum* cells as model system for studying eukaryotic cell migration in DC electric fields. We have defined the temporal electric persistence to characterize the memory that cells have in a varying electric field. In addition to imposing a directional bias, we observed that the electric field influences the cellular kinematics by accelerating the movement of cells along their paths. Moreover, the study of vegetative and briefly starved cells provided insight into the electrical sensing of cells. We found evidence that conditioned medium of starved cells was able to trigger the electrical sensing of vegetative cells that would otherwise not orient themselves in the electric field. This observation may be explained by the presence of the conditioned medium factor (CMF), a protein secreted by the cells, when they begin to starve. The results of this study give new insights into understanding the mechanism that triggers the electrical sensing and transduces the external stimulus into directed cell migration. Finally, the observed increased mobility of cells over time in an electric field could offer a novel perspective towards wound healing assays.

Introduction

Electrotaxis, also known as galvanotaxis, is the directed migration of biological cells in a DC electric field. Since it was first described over a century ago [1, 2], the electrotactic behavior of various cell types, including cancer cells, neurons, fibroblast, keratinocytes, leukocytes, endothelial and corneal epithelial has been reported [3–12]. Electrotaxis is thought to be involved in a wide range of physiological processes, such as embryogenesis, neuronal guidance, wound healing, and metastasis [13–18]. Recently, also *Dictyostelium discoideum* (*Dd*), the social amoeba well-known as a model for studying cell motility and chemotaxis [19] has proven to be

a suitable model for investigating electrotaxis [20–22]. However, the mechanism triggering the local activation of the signal transduction cascade that leads to actin polymerization and membrane protrusion and more generally the mechanism underlying the directed cellular movement of *Dd* cells in the electric field still awaits clarifications.

A study on the involvement of cAMP receptors using $cAR1^-$ - $cAR3^-$ cells showed that *Dd* cells, which are unable to sense cAMP, are electrotactically as efficient as wild type cells [21]. The same study showed that the cAMP binding transduction unit constituted by the *Gα2* subunit and *Gγβ* complex does not play any role in the transduction of the extracellular electric signal into directional movement. Indeed, like $cAR1^-$ - $cAR3^-$, $Gα2^-$ and $Gβ^-$ mutants also exhibit sustained electrotaxis albeit with a reduced migration speed [21].

Another molecular study identified the genes required for the directional switching of electrotactic migration.

By genetically modulating both guanylyl cyclases (GCases) and the cyclic guanosine monophosphate (cGMP)-binding protein C (GbpC) in combination with the inhibition of the phosphatidylinositol 3-kinases (PI3Ks) the cells reversed their directed migration from the cathode to the anode [23]. Gao et al. [24] uncovered genes involved in the electrotactic response by identifying 28 strains with defective electrotaxis and 10 strains with a slightly higher directional response. They showed *PiaA* to be an essential mediator of electrotaxis. This gene encodes a critical component of TORC2, a kinase protein complex that transduces changes in motility by activating the kinase PKB. Furthermore, they identified several genes that encode other components of the TORC2-PKB pathway (*gefA*, *rasC*, *rip3*, *lst8*, and *pkbR1*) in playing important roles in the signalling pathway for electrotaxis. While genes and proteins that mediate electrical sensing and define the migration direction have been investigated in *Dd* cells, the cellular kinematic effects caused by electric field, as well as the initial trigger mechanism of electrical sensing still present many riddles.

In this study we characterize the effect of electric fields on cells in terms of migration velocity and directionality as a function of time. In addition, we introduce the concept of electrical persistence to investigate how cells invert their trajectory when the electric field is reversed. We also studied the response of vegetative *Dd* cells and observed that the presence of conditioned medium helps them to sense the electric field and orient themselves towards the cathode. We focus our attention on the conditioned medium factor (CMF), a protein that *Dd* cells secrete when they begin to starve, as a possible trigger of the cellular electrical sensing. CMF has been shown to coordinate aggregation by regulating several aspects of cAMP signal transduction such as the activation of Ca^{2+} influx, adenylyl cyclase, GCases, and gene expression [25, 26]. Besides influencing cAMP signalling, CMF also participates in regulating cell shape. Moreover, cell migration relies on pseudopod formation, and CMF appears to allow cells to create pseudopodia more frequently than cells without CMF in their surroundings [27]. CMF is therefore a reliable candidate for such a triggering task.

Materials and methods

Cell preparation

Wild type, *LimE-GFP*, *ACA^-*, and *Amib^-* were cultivated in HL5 medium (Formedium) at 22°C on polystyrene Petri dishes (Primaria, Falcon, BD Becton Dickinson) or shaken in suspension at 150 rpm. As long as nutrients are available (HL5 medium), *Dd* cells proliferate as unicellular amoeba and are defined as vegetative cells. When the cells deplete their food source and start to starve (in our case, the HL5 medium is removed and replaced by buffer), they enter a developmental cycle. For preparation of experiments, cells were starved in shaking phosphate buffer (PB, 2 g KH_2PO_4 and 0.36 g $Na_2HPO_4 \cdot 2H_2O$ per 1 L, pH 6) for different

durations according to the corresponding experiment. For assays with developed cells, they were starved for 1h, 5h, 6h, 8h at a density of $\sim 2 \times 10^6$ cells/mL. The shaking culture was pulsed with 50 nM cAMP (Sigma) every 6 min over the course of the starvation time when the experiment required it. After the corresponding starvation time with or without cAMP pulses, the cells were harvested and washed in PB. An aliquot of the cell suspension was injected into the chamber for the electrotactic assay, and the cells were allowed to spread on the glass substrate for 15 min at 22°C. During this time a PB flow of 30 μ l/h was applied by a syringe pump (Harvard Apparatus, PHD 2000) to the cells in order to wash away the cAMP produced by the cells. It was switched to 50 μ l/h during the experiments. For experiments with vegetative AX2 cells the cells cultivated in HL5 medium were detached from the Petri Dish bottom, washed twice with PB and put directly into the experimental chamber without any additional starvation time. For the experiment with conditioned medium AX2 cells were shaken for 1 h without the addition of cAMP. They were centrifuged, the buffer was harvested and centrifuged twice again to eliminate possible cells. The vegetative cells after having been detached from the Petri Dish were washed and afterwards resuspended in the conditioned buffer. All cell lines were derived from the axenically growing strain *Dictyostelium discoideum* AX2. Wild type and LimE-GFP cells were kindly provided by G. Gerisch (Max Planck Institute for Biochemistry, Martinsried, Germany). ACA⁻ were kindly provided by A. Kortholt (University of Groningen, Netherland), Amib⁻ cells were bought from Dicty Stock Center of dictyBase (dictybase.org).

Microfluidic device

Fig 1A illustrates the design of the custom-made microfluidic device used during the experiments. Standard soft lithography was used to produce microfluidic channels 1.5 mm wide, 100 μ m high, and 30 mm long. A master mold was fabricated by transferring via photolithography a pattern to a layer of photoresist (SU-8, Micro Resist Technology), spin coated on Si wafer (Si-mat, Germany). To obtain the microfluidic device, polydimethylsiloxane (PDMS, 10:1 mixture with curing agent, Sylgard 184, Dow Corning Europe SA) was poured onto the wafer and cured for 45 min at 75°C. A PDMS block containing the channels was cut out, inlets and outlets for the PB washing flow were punched through the PDMS by using a syringe tip and two holes with a diameter of 6 mm were punched at the two ends of the channels in order to insert the agar bridges. A glass coverslip (24x60 mm, #1.5, Menzel Gläser) was sealed to the PDMS block after a 20 sec treatment in air plasma (PDC 002, Harrick Plasma) to close the channels.

Electric connection

The channel was connected to the power supply through 2% agar salt bridges 13 cm long. They were prepared in custom-made glass tubes with an internal diameter of 3 mm (Glasgeraetebau Ochs, Germany) filled with PB supplemented with 2% (w/v) agar. One side of the agar bridge was inserted into the 6 mm diameter hole at the end of the channel, and the other side was placed into buffer reservoirs filled with PB. Ag/AgCl electrodes were immersed into the reservoirs in order to close the circuit channel-power supply. The Ag/AgCl electrodes (12 cm) were prepared by immersing two silver wires (99.9%, 1mm in diameter, Windaus Labortechnik, Germany) in household bleach for one hour. A programmable switch device (Siemens) was set to reverse the polarity of the electric field every 30 min within a few milliseconds. The resistance of the channel was 840 K Ω and the flowing current 25 μ A. Upon the application of direct current voltage of 10 V/cm, we measured that an electric field of 7 V/cm was applied to the cells. This voltage drop was due to the agar bridges that we used to connect the channel with the power supply generator in order to avoid the harmful effects of the electric field on the cells, i.e. ions generated by electrolysis, changes in pH value, air bubble formation.

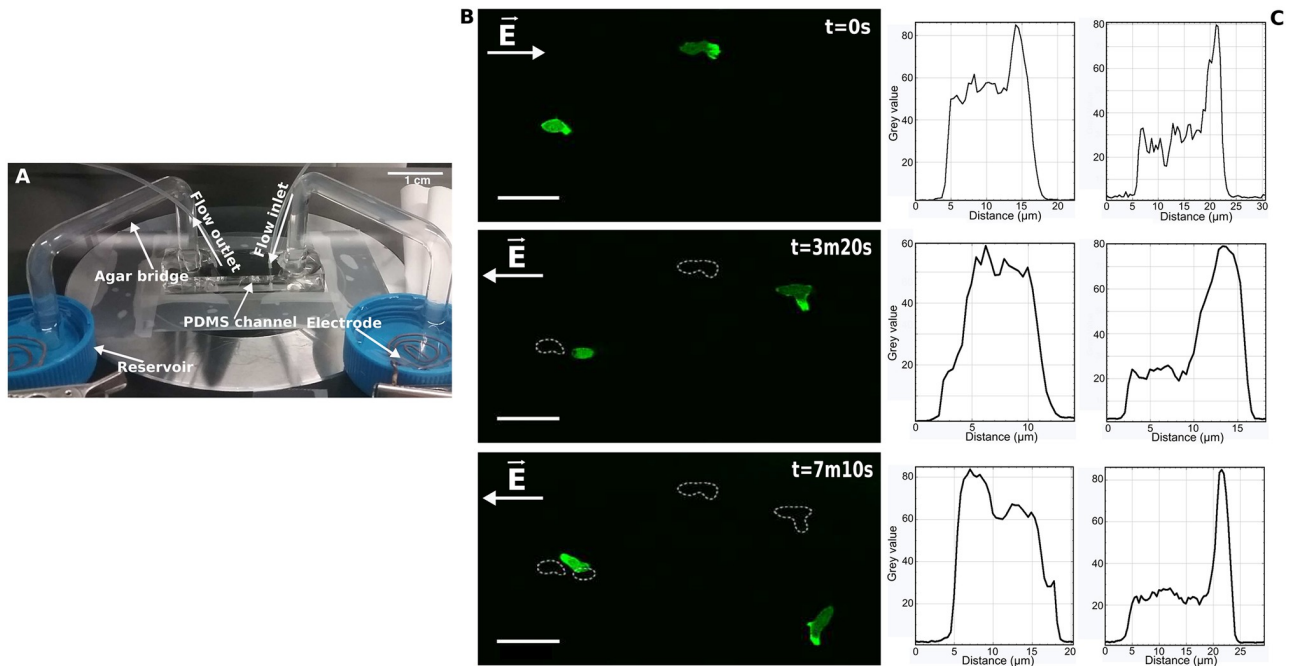


Fig 1. Experimental set up and F-actin polymerisation. A. Experimental set up. The electric field in the channel is generated through an indirect contact with the electrodes. The buffer reservoirs provide the electric connection between electrodes and agar bridges (for more technical details refer to Materials and Methods section). B. F-actin polymerisation through LimE-GFP. Cells with different morphology use different strategies to reverse their trajectory when the polarity of the electric field changes. The cell on the left rounds, extends a pseudopod in the new direction and forms a new leading edge whereas the cell on the right reverses its trajectory by doing a U-turn. The dashed lines show the changing position of the two cells. Scale bar: 25 μm . C. Histograms of fluorescence intensity within the cell representing the localization of F-actin. Distance refers to the gap from the center of the cell's leading projection through the cell body (see S1 Fig in S1 File). The left and right graphs correspond to the cells on the left and the right of the picture, respectively. The change in position of F-actin from the front to the back in the cell on the left when the electric field is reversed is clearly visible, while in the U-turn cell the F-actin remains at the front.

<https://doi.org/10.1371/journal.pone.0239379.g001>

Microscopy and cell mobility analysis

The cells in the microfluidic channel were observed with an inverted microscope (Olympus IX-71) in bright field with a DeltaVision imaging system (GE Healthcare), while the migration of the cells were recorded with a CCD camera (CoolSnap HQ2, Photometrics). Data acquisition started 20 sec after the application of electric field. Cell images were acquired every 20 s for 2 hours. In the experiments with cells developed for 5–8 h cell centroids were determined manually, and the trajectories of the cell centroids were traced using MTrackJ, an ImageJ/Fiji plugin. The trajectory velocity was calculated by dividing the total path length of cell migration by the time interval. The cellular velocity was presented as the mean value of the velocities of the cells recorded in each 30-minute time interval. Directionality of a cell with respect to the electric field, representative of the efficiency of the cell to migrate toward the cathode, was defined as $\cos\theta$, where θ is the angle between the vector connecting the starting and ending point of the cell trajectory and the field line of the electric field. It was calculated every minute. For the visualization of the F-actin localization, the cell contours were automatically detected using the method described in [28]. The center of mass of cells CM and the intensity-weighted center of mass CM_W were computed considering the intensity of the pixels representing the actin localization. Every 20 seconds we considered that cells were moving toward the direction of the electric field when the vector $CM-CM_W$ was pointing towards the cathode. When that vector was pointing in the opposite direction, we considered the cells moving anti-parallel to

the electric field (see S1 Fig in [S1 File](#)). The cell's locations are acquired every 5 seconds and the bins in Figs 4B and 5B represent the average number of cells moving parallel or antiparallel to the electric field every 20 seconds (also considered as the error over 4 frames). At the early or late phase of the experiment the number of cells is smaller than in the rest of the time. This is due to cells entering or leaving the field of view during visualization that could not be tracked for the entire observational time. We therefore restricted the analysis to times when the cells number is approximately constant. Also in the experiments with vegetative and briefly starved cells, cell contours were automatically detected using the method described in [28]. The cell centroid was then computed and with a time interval of 20 sec between subsequent frames its position was tracked using a custom-made MATLAB program.

Results and discussion

In this study we present results on the movement of *Dd* cells in DC electric fields. We focus our analysis on the effects of electric fields on the cell kinematics and on the cellular tendency to maintain the direction of motion imposed by the electric field. We show how these effects are reflected in the actin polarization process. Lastly we present the electrotaxis of vegetative and briefly starved cells and suggest a possible mechanism regulating the electric sensing independently from the cAMP-induced development.

Electrotaxis of developed starved cells

We investigated the response to the electric field of AX2 starving wild-type cells developed for 5 hours under cAMP pulsing prepared with the same development procedure as used for the study of chemotaxis (see [Materials and methods](#) section). The cells were seeded into a microfluidic channel where the electric field was applied for two hours. The geometry of the channel guaranteed a uniform electric field with parallel field lines along the channel ([Fig 1A](#)). Under the influence of an electric field of 7 V/cm cells polarized and exhibited migration towards the cathode. We chose not to apply voltages as high as reported by other studies (up to 20 V/cm) [20, 21, 24, 29] in order to reduce the Joule heating and the associated temperature increase towards non-physiological conditions (see [Materials and methods](#)). We observed a high cellular death rate for voltages above 13 V/cm; as a result, we restricted our investigation to 7 V/cm. After exposing the cells to 7 V/cm for two hours we observed no change in cellular viability and behaviour. This we tested by removing the electric field and the flow in the microfluidic device after the experimental time and verified that subsequently the cells aggregated and followed the natural life cycle.

In order to remove the cooperative effects of cAMP signalling of the wild-type *Dd* cells, a flow of phosphate buffer (PB) with a flow speed of 100 $\mu\text{m/s}$ [30] parallel or antiparallel to the electric field lines was applied. The successful removal of any extracellular signalling molecule was confirmed by the absence of cell aggregates during the experiments, which would occur for *Dd* cells developing normally. The flow speed was adjusted such that the mechanical shear had no effect on the directed motility of the cells. In our case we calculated the shear stress to be 6 mPa, a value well below the critical shear stress for mechanotactical response (0.8 Pa) [31, 32]. We also verified the effect of electro-osmotic flow on the cell motility. We analysed the movement of beads with a diameter of approx. 1 μm in the flow induced by electro-osmosis. The velocity of the beads was found to be around 8.8 $\mu\text{m/s}$, i.e., much smaller compared to the velocity of the external applied flow. Therefore the effect of the electro-osmotic flow on the cell migration can be neglected. Altogether, this shows that the directed migration elicited by the electric field in our experiments was not influenced by external factors such as the applied flow, electro-osmotic flow, or chemical gradients.

We also found no evidence that extracellular Ca^{2+} is necessary for electrotaxis. The experiments presented here were conducted with Ca^{2+} -free phosphate buffer. Moreover, the flow in the microfluidic device washes away any compound released by the cells. This evidence contradicts the results by Shanley et al. [33], where it was found that electrotaxis was not possible in the absence of extracellular Ca^{2+} .

When the electric field polarity was reversed, the cells turned around and migrated towards the new cathode (See [S1 Movie](#)), confirming the observations reported by [20, 22]. In response to inverting the field polarity the cells reversed their trajectory by using two different strategies, depending on their initial morphology: In most cases polarised cells with a single pseudopod or an accentuated pseudopod achieved reorientation by making a U-turn while maintaining their morphological polarity. Cells with a less polarised initial morphology reoriented by forming extensions of the pseudopod in the direction of the new cathode, i.e. reversing the front and the rear. With LimE-GFP as an in-vivo marker for F-actin we visualised the distribution of actin during this process. [Fig 1B](#) (see also [S2 Movie](#)) shows an example of cells with the two different cellular morphologies: the U-turn cell shows strong localisation of F-actin at the leading pseudopod, while it is less pronounced in the other cell. In response to the polarity change of the field, the U-turn cell retains its F-actin localisation, while in less polarized cells F-actin is redistributed from back to front, forming a new leading edge. This behaviour was also observed during chemotaxis [34] and demonstrates that the electric field triggers migration by activating the molecular signalling pathway that transduces an external stimulus into the actin polymerisation. Therefore, an intracellular electric polarization due to passive electrostatic effects of the electric field can be excluded. Additionally, we have observed that the cells become tapered over time and thus the U-turn strategy, typical for polarized cells, becomes the observed reversal strategy.

Cellular velocity, directionality and temporal electric persistence. When the cells were exposed to the electric field for two hours, with the field reversing every 30 minutes, we observed that the migratory velocity increased continuously during the observation period. The increasing length of the cellular trajectory over time is clearly visible in [Fig 2](#), and the corresponding cell velocity increases from $3.27 \pm 0.2 \mu\text{m}/\text{min}$ in the first 30 minutes to $8.3 \pm 0.4 \mu\text{m}/\text{min}$ after 2 hours ([Fig 3C](#)). To investigate whether this observation depends on the stage of development induced by the cAMP pulsing procedure, we tested the response of cells that were starved and pulsed for 5, 6 or 8 hours. The cell speed for the case of 6 and 8 hours is shown in [Fig 3A and 3B](#). The acceleration of the cells caused by the electric field was also observed in these cases and calculated as $a = \Delta v / \Delta t$, with Δv the difference in velocities between time intervals and Δt the time interval of 30 minutes. [Fig 3D](#) shows that the three cell populations reacted to the electric field with an increase of the initial velocity, regardless of their developmental stage. We speculate that the cAMP pathway involved in the activation of the aggregation adenylyl cyclase (ACA) and associated production of cAMP could play a significant role. In fact, we observed that two mutant strains unable to produce cAMP and aggregate, namely ACA^- and Amib^- , did exhibit electrotaxis, but did not show any increase in velocity over time (See [S3 Fig](#) in [S1 File](#)). Nevertheless at this stage this assumption is a speculation and only a detailed molecular study similar to [24] can elucidate the true reason for the speed up.

Interestingly, the directionality of the cells did not change significantly ([Fig 4A](#)) reaching a plateau value Dir_{max} which ranged from 0.54 in the first 30 min to 0.65 in the last interval. By reversing the electric field every 30 minutes we were able to observe how the cells adapt to the electric field over time, and the transition phase between two plateaus provides information about the reaction of cells to the reversal of the polarity of electric field. In fact, the cells showed a faster reaction in the first interval, which slowed down and stabilized after the second

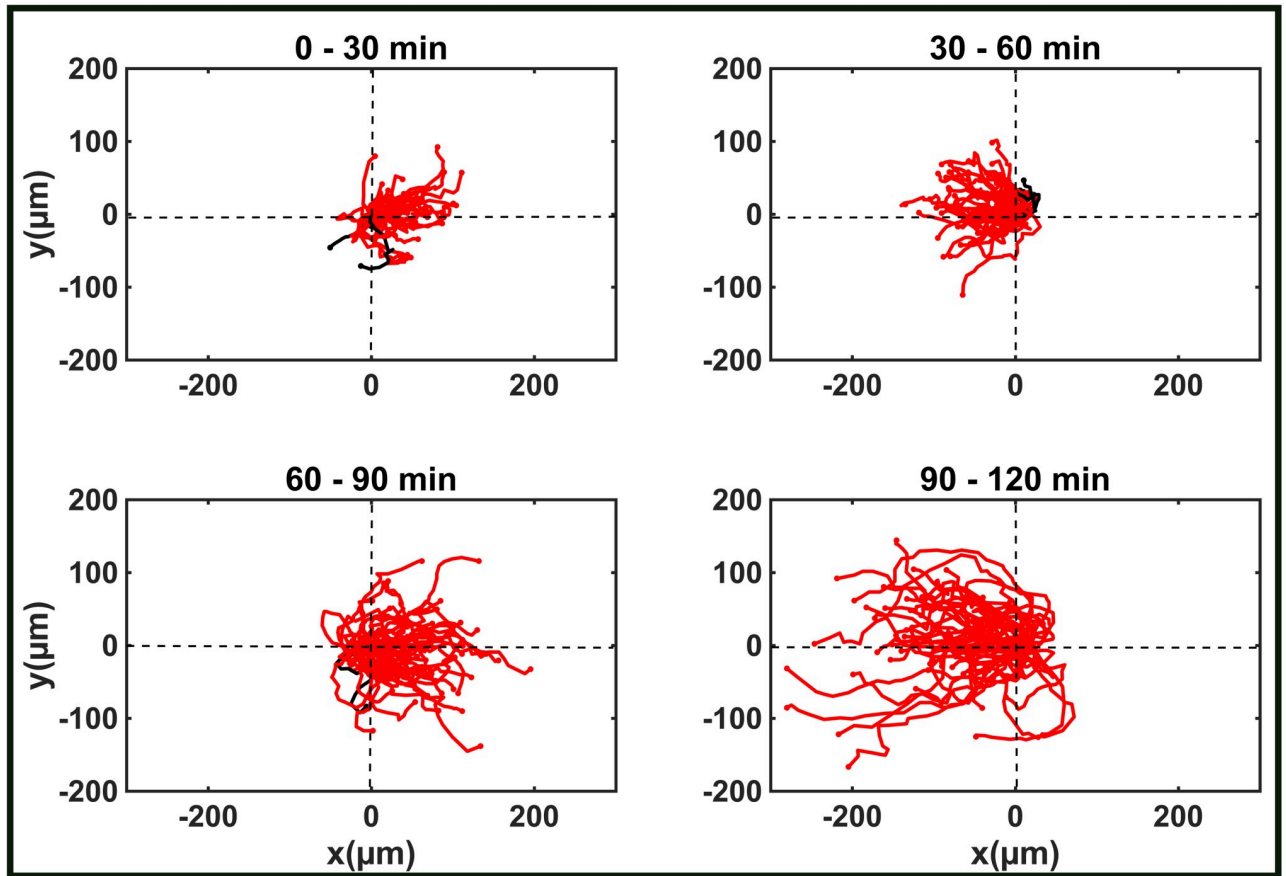


Fig 2. Cell tracking diagrams of fully developed AX2 cells. The length of the migration paths increases significantly over time. In each experiment at least 45 cells were analysed. The diagrams refer to cells that were starved for 5 hours. They originated from at least three different experiments.

<https://doi.org/10.1371/journal.pone.0239379.g002>

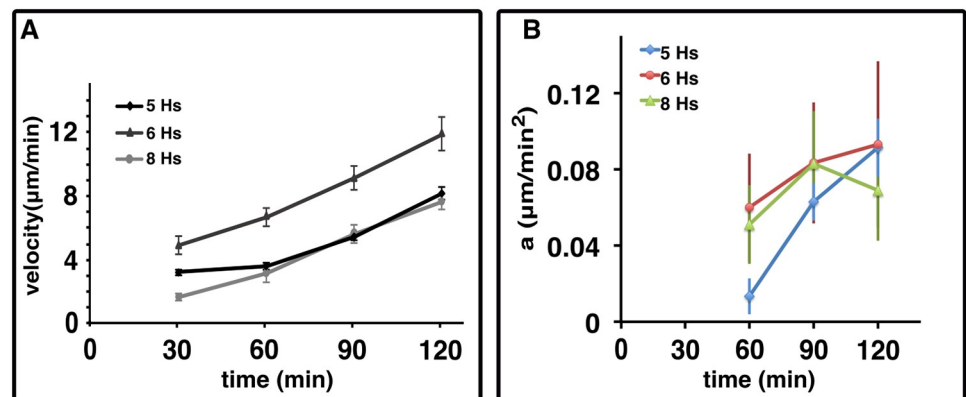


Fig 3. Cell acceleration. A. Migration velocity of Ax2 cells starved for 5, 6, and 8 hours. B. Cell acceleration over time for cells starved and pulsed 5, 6 or 8 hours. All data are represented as *mean* ± *s.e.m.*

<https://doi.org/10.1371/journal.pone.0239379.g003>

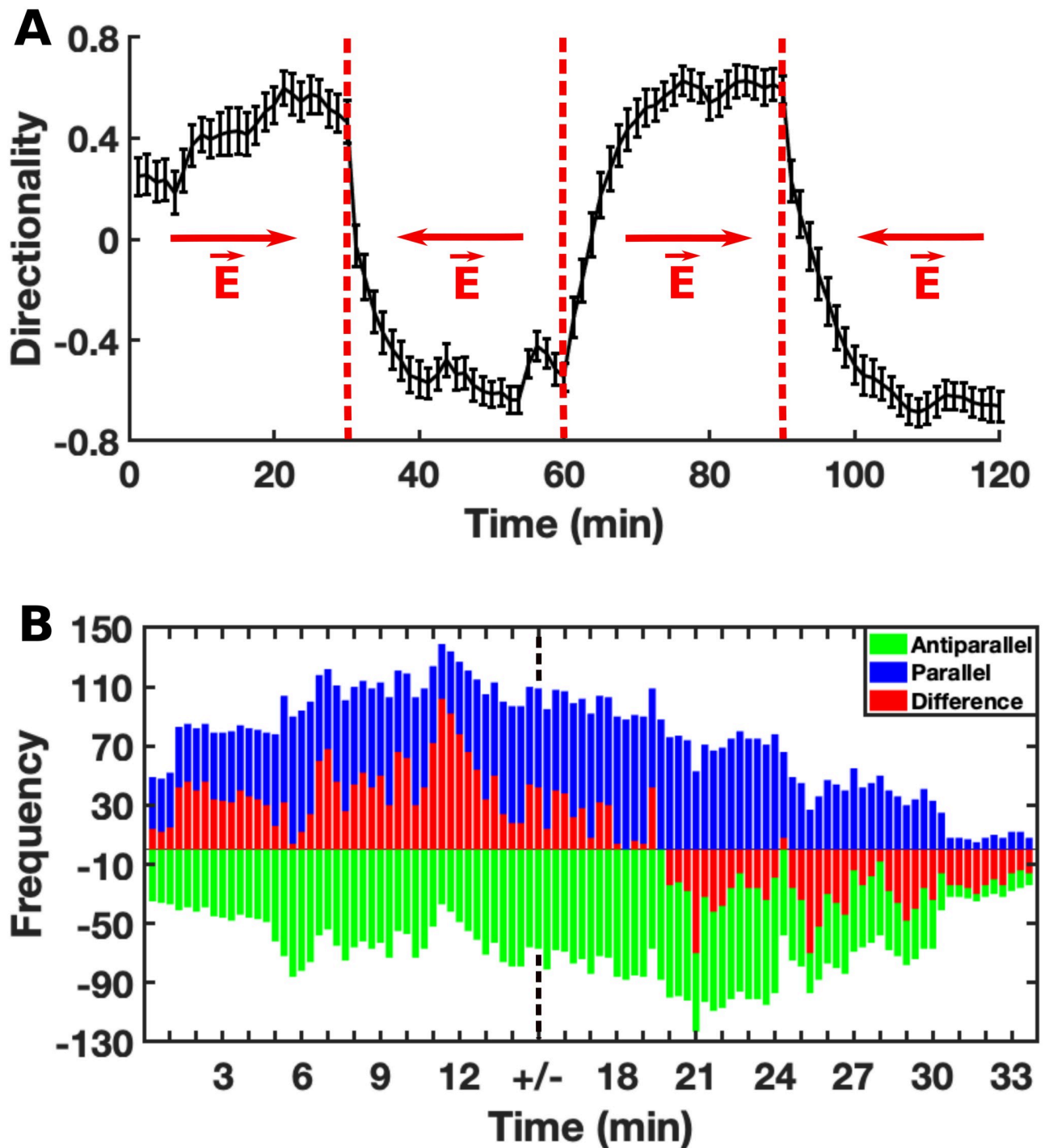


Fig 4. Directionality and F-actin localization upon electric field reversal. A. Directionality of *Dd* cells in an electric field. The polarity of the field is reversed every 30 minutes as indicated by the red arrows. The graph is obtained from at least three different experiments. The data are displayed as *mean*±*s.e.m.* B. F-actin localization within the cell during cellular migration and its dynamics when the polarity of the electric field changes. At each point in time, the number of cells with F-actin localized towards the cathode (blue), towards the anode (green) and their difference (red) are displayed. The black dotted line indicates the time point of polarity reversal.

<https://doi.org/10.1371/journal.pone.0239379.g004>

interval. By fitting this cells response to the exponential function $Dir_{max} - ce^{\frac{t}{\tau}}$ we calculated that it is characterized by a time constant $\tau_{30-60} = 2.94$ min in the first electric field reversal, followed by $\tau_{60-90} = 5$ min and $\tau_{90-120} = 5.64$ min in the second and third one, respectively (where the subscript of τ refers to the corresponding time interval in minutes). It appears clear that the longer the cells are under the influence of the electric field, the longer it takes for them to reverse their trajectory when the polarity of the electric field is reversed. Thus, the adaptation to their environment prevents the cells from reacting immediately to any change in the electric field and rearranging the migratory machinery. To characterize this behavior, we defined the temporal electrical persistence or electrical memory, i.e. the time required by cells to reverse their trajectory in an inverted electric field. In this way, we could gain insights into the cellular sensing process and its transduction into the molecular pathway. For this purpose we analyzed the localization of the F-actin network by using LimE-cells and we could observe how the adaptation behavior was reflected by F-actin polymerization inside the cell. The cells were kept in the electric field for 90 minutes. Afterwards, the polarity was reversed and the cells were observed for 20 minutes (Fig 4B). We evaluated the occurrence of cells in which F-actin was localized towards the cathode and of cells in which it was localized in the opposite direction. The difference between these two populations represents the net population of cells polarized in the direction defined by the electric field (see section [Materials and methods](#) for analysis details). These results show that the cells need $4.3 \text{ min} \pm 20 \text{ sec}$ to shift the F-actin in the new direction of the electric field after the polarity change. To better characterize the sensing mechanism, we analysed the temporal electrical persistence of the cells when the electric field was removed and tested how long it took for the cells to “forget” the environmental stimulus and move randomly. Cells migrating without any electrical stimulus showed no preferred direction (Fig 5A), and the average directionality of their random movement was 0 ± 0.2 . We measured the temporal electrical persistence of cells without electrical influence after they were kept in the electric field for 90 minutes (Fig 5A). We saw that the cells without electrical influence reduced their directionality towards the electric field and showed random movement after a period of 6 minutes. By visualizing the F-actin we could observe that the time needed to completely lose polarization and not to show preferred localization of F-actin was $9.2 \text{ min} \pm 20 \text{ sec}$ (Fig 5B). Also in this case we could observe that the directed movement decreased with time when the electric stimulation was switched off.

Electrotaxis of initially vegetative cells

In this study we were also interested to understand the mechanism involved in the initiation of the electrical sensing in cells. For this purpose we analysed the behaviour of vegetative and briefly starved *Dd* cells under the influence of electric fields. It allowed us to study the response of cells before they entered the development phase and went through the program of gene-expression changes induced by cAMP pulses.

Vegetative wild type AX2 cells cultivated in HL5 medium were washed and resuspended in PB, then seeded immediately into the microfluidic device. We analysed their behaviour under the influence of electric fields over a period of up to 7 hours, during which the polarity of the electric field was reversed every 30 minutes. No directed movement was observed; rather, the cells migrated randomly during the whole observation time. Fig 6A shows the behaviour of vegetative cells in the electric field for 2 hours. After 7 hours deprived of nutrients in PB the cells did not show the typical characteristics of starved cells in an electric field such as morphological changes and migration towards the cathode. As a control experiment, we tested the effect of the electric field on cell physiology and repeated the experiment by keeping the cells under the flow for 5 hours without electric field and then applying the electric field for 2 hours.

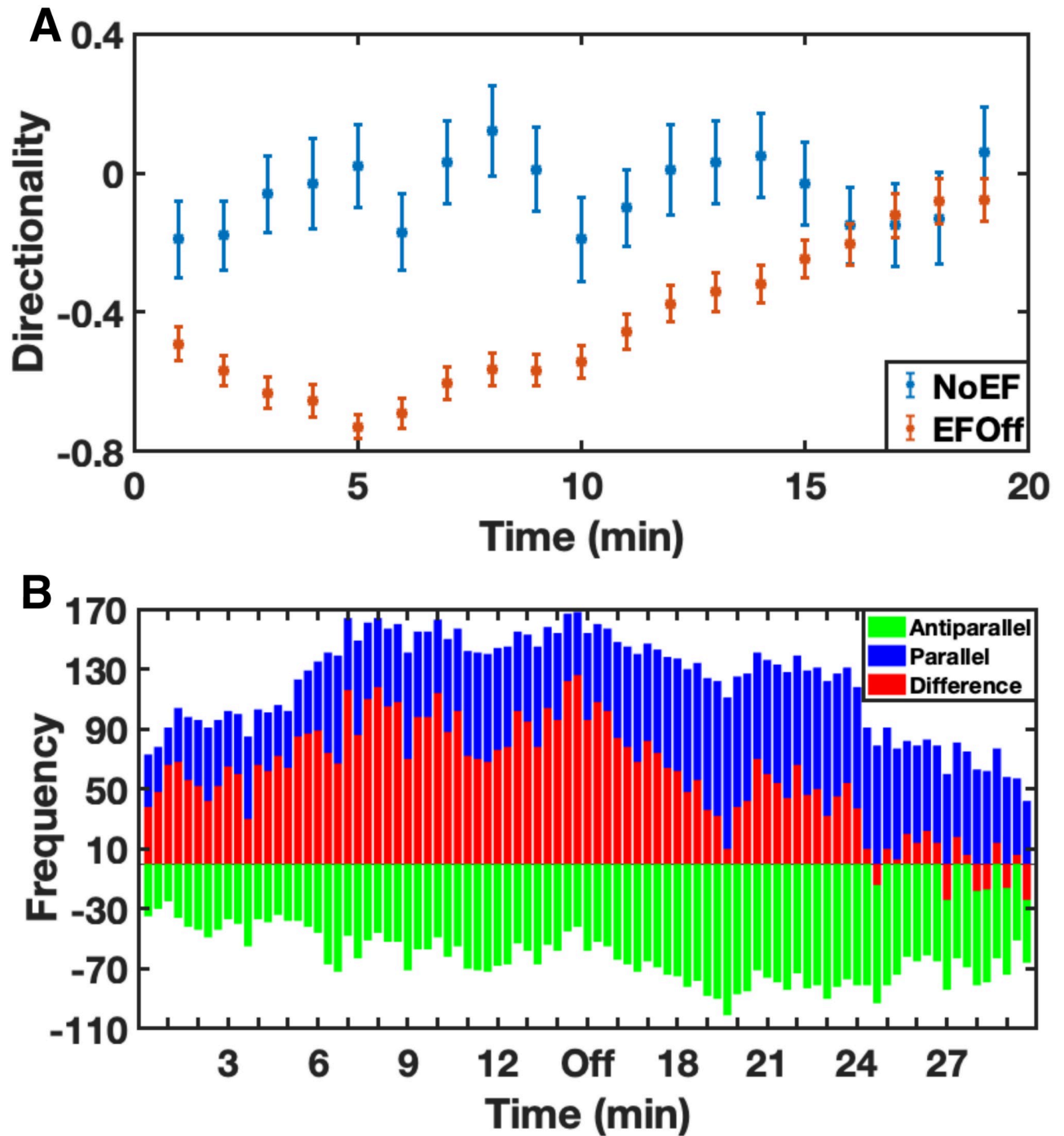


Fig 5. Electrical persistence without electric field. A. Directionality of *Dd* cells that were never exposed to electric field and move randomly (blue) and cells where the electric field was switched off after 90 min (red). The electric field was removed at $t = 10$ min. It is clear that the directionality decreases during the time after the field removal. The data are represented as $mean \pm s.e.m.$ B. F-actin localization inside the cell during the cellular migration and its dynamics when the electric field is switched off.

<https://doi.org/10.1371/journal.pone.0239379.g005>

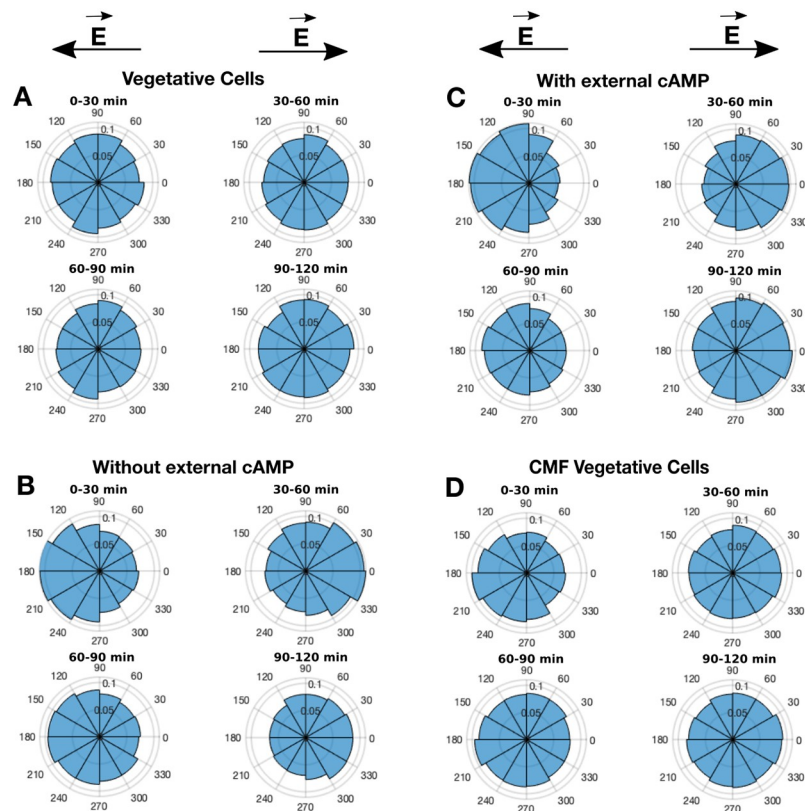


Fig 6. Polar histograms of the propagation angle distribution. Polar histograms of the propagation angle distribution for vegetative cells (A), briefly starved cells in a shaking culture without (B) and with (C) external cAMP pulses, and conditioned vegetative cells (D). Cell motion is biased towards the cathode with $\theta = 180^\circ$ in the first 30 min and $\theta = 0^\circ$ or 360° when the polarisation of the electric field has been reversed. The histograms represent the distribution of the propagation angle $\theta \in [0^\circ, 360^\circ]$ of each time step with respect to the electric field lines pointing towards the cathode. Every histogram resulted by the analysis of 100–300 cells from three different experiments.

<https://doi.org/10.1371/journal.pone.0239379.g006>

Again, the cells showed no preferred direction of movement. In order to check the involvement of calcium (Ca^{2+}) in this behaviour we repeated the experiments by substituting the Ca^{2+} -free PB for a buffer containing 1mM CaCl_2 . No remarkable difference was observed in the cells response to the electric field. We concluded that under these experimental conditions the cells were not able to enter the developmental stage normally induced by starvation. Thus, entering the developmental phase and activating genes related to the starvation program are necessary steps for enabling cells to sense and respond to the electric field.

Electrotaxis of briefly starved cells

The influence of the initial starvation on the behaviour of cells in electric fields was investigated by experiments with cells starved for 1 hour both with and without additional cAMP pulses in shaking culture (see [Materials and methods](#)). We observed that cells starved for 1 hour with and without additional cAMP pulses reacted similarly by migrating or realigning their cell body towards the cathode when the electric field was applied for 30 minutes. They inverted their orientation towards the new cathode when the polarity of the electric field was reversed ([Fig 6B and 6C](#), see also S4 Fig in [S1 File](#)).

Interestingly, after one hour the directed movement decreased with time, independent of the change in the polarization of the electric field. As in the case of vegetative cells, we repeated these experiments using a buffer containing 1mM CaCl₂ as washing out flow. Again, no difference in the attenuation effect after 1 hour was observed.

These results show that the induction of development by nutrient deprivation leads to an increased electrotactic capacity, but not the presence of exogenous cAMP. This is not surprising since Yuen et al. have shown that the ability of cells to transduce external cAMP occurs 2 hours after starvation [25].

Conditioned medium restores the cellular sensing for external electric stimuli

So far we have observed a difference in electrical sensing between vegetative and 1-hour-starved cells. We verified that the presence of external cAMP is not essential for triggering the electrical sensing of cells. We therefore assume that the electrical sensing is triggered by a signaling molecule that the cells immediately release at the onset of starvation. In order to test this hypothesis, we studied the reaction of vegetative cells to electric fields when they were resuspended in conditioned medium. We starved wild-type cells in a shaking culture for 1 h, centrifuged them, removed the conditioned buffer and used this conditioned medium to resuspend vegetative cells. These conditioned vegetative cells were immediately seeded into the microfluidic channel and conditioned medium was also used as washing flow instead of PB during the entire observation period of 2 hours. Interestingly, under these conditions the conditioned vegetative cells showed an electrotactic motion and reoriented their cellular body towards the cathode during the first 30 minutes. Fig 6D clearly shows the reaction of the cells to the electric field. The involvement of conditioned medium in the electrical sensing and its triggering effect is clearly visible when comparing the cellular response of the initially vegetative cells (Fig 6A) and the conditioned vegetative cells (Fig 6D). By comparing the reactions to the electric field of the conditioned vegetative cells (Fig 6D) and the briefly starved cells (Fig 6B and 6C), we can see that conditioned medium rescues the sensing of cells for electric fields, but the cells lose their electrotactic response with time, i.e., after the first 30 minutes, the cells' responsiveness to the electric field disappeared.

Although there are dozens of autocrine agents in the conditioned medium of cells starved for only one hour, we speculate that the decisive factor triggering the cellular electrical sensing is the conditioned medium factor (CMF) [25], a protein that the cells release at the onset of starvation. It is secreted throughout development by *Dd* cells, but not by vegetative cells [35]. Various studies suggest that CMF is essential for cell-cell communication and for the coordination of cell aggregation. It acts during the earliest stages of starvation and is used by the cells to enter the developmental phase and induce the expression of selected genes depending on the spatial density of cells [26, 36].

While conditioned vegetative cells immediately showed electrotaxis, vegetative cells were not able to sense the electric field when seeded in a channel with a PB flow up to 7 hours. We attribute this behavior to the flow that washes away not only cAMP but also the CMF secreted by the cells. Under these conditions they cannot enter the developmental phase. According to our hypothesis, CMF receptors might be responsible for the signal transduction of the external electric field and thus for the activation of the signaling pathways that lead the cells to polarization and directed migration. It is known that the gene encoding CMF receptors is expressed in vegetative cells and CMF receptors accumulate on the cell membrane when starvation sets in [37]. In addition, CMF binds to CMF receptors and regulates PldB [27], a phospholipase D homologue known to regulate actin localization [38] and pseudopod formation [27], which

are essential for cell migration. This is consistent with the fact that in our microfluidic experiments vegetative cells did not show any electrotaxis, while briefly starved cells and conditioned vegetative cells were electrotactic. The temporal decrease in electrotactic directionality in all three cases may be attributable to the lack of increase in CMF.

Conclusion

In this study we present results on the electrotactic behavior of *Dd* cells at different developmental stages. We showed that fully developed wild-type *Dd* cells respond to the electric field by increasing their migratory velocity over time. However, the mutant strains *ACA*⁻ and *Amib*⁻ migrate at a constant velocity over the observation period. At this stage it is unclear whether the enzyme *ACA*, which is known to be essential for oscillatory cAMP signals, is involved in the determination of the electrotactic migratory velocity. Nevertheless, this result suggests that the mechanisms that regulate the increase in migratory speed and the electric sensing may be different. We introduced the temporal electrical persistence as the time delay of cells to respond to the variation of the external electric field. We quantified the time interval in which the cells rearrange their migratory machinery either to reverse their migratory trajectory or to “forget” the electric stimulus after switching off of the field. This provides insight into the mechanism by which cells transduce the sensing of the electric stimulus into a kinematic response. By analysing vegetative cells that are not capable of directed movement, we show that the electric sensing can be rescued by using conditioned medium. We believe that among the autocrine molecules that the cells release at the onset of starvation, CMF is the prime candidate for triggering the electrical sensing. Only when cells have been exposed to CMF (self-produced or supplied with conditioned medium) do they respond to the electric field with directed migration. This assumption requires an analysis using the protein CMF instead of the conditioned medium. Until now, the protein could not be made available to test our assumption. We encourage researchers to follow this line of inquiry.

Supporting information

S1 File.

(PDF)

S1 Movie. Electrotaxis of wild type AX2 *Dd* cells. The cells starved 5 hours with cAMP pulses. The images were acquired every 20 s for 2 hours and the polarity of the electric field was reversed after 60 minutes.

(AVI)

S2 Movie. Visualization of F-actin distribution under the influence of the electric field.

AX2 *Dd* cells starved for 5 hours with cAMP pulses. The images were acquired every 10 s for 10 minutes and the polarity of the electric field was reversed after 5 min.

(AVI)

Acknowledgments

We acknowledge Albert Bae, Narain Karedla, and Christian Westendorf for fruitful discussion and suggestions; Maren Müller, Katharina Gunkel, Achim Hillebrandt, and Riccardo Guido for technical support.

Author Contributions

Conceptualization: Isabella Guido, Eberhard Bodenschatz.

Data curation: Isabella Guido.

Formal analysis: Isabella Guido, Douglas Diehl, Nora Aleida Olszok, Eberhard Bodenschatz.

Funding acquisition: Eberhard Bodenschatz.

Investigation: Isabella Guido, Douglas Diehl, Nora Aleida Olszok.

Methodology: Isabella Guido.

Project administration: Isabella Guido.

Supervision: Isabella Guido, Eberhard Bodenschatz.

Validation: Isabella Guido.

Visualization: Isabella Guido, Douglas Diehl, Nora Aleida Olszok.

Writing – original draft: Isabella Guido.

Writing – review & editing: Isabella Guido, Douglas Diehl, Eberhard Bodenschatz.

References

1. Dineur E. Note sur la sensibilité des leucocytes à l'électricité. *Bull Seances Soc Belge Microsc.* 1891; 18:113–118.
2. Verwon M. Untersuchungen über die polare Erregung der lebendigen Substanz durch den konstanten Strom. *Mittlung Pflügers Arch Eur J Physiol.* 1896; 62:415–450. <https://doi.org/10.1007/BF01790002>
3. Djamgoz MBA, Mycielska M, Madeja Z, Fraser SP, Korohoda W. Directional movement of rat prostate cancer cells in direct-current electric field. *Journal of Cell Science.* 2001; 114(14):2697–2705.
4. Fraser SP, Diss JKJ, Chioni AM, Mycielska ME, Pan H, Yamaci RF, et al. Voltage-Gated Sodium Channel Expression and Potentiation of Human Breast Cancer Metastasis. *Clinical Cancer Research.* 2005; 11(15):5381–5389. <https://doi.org/10.1158/1078-0432.CCR-05-0327> PMID: 16061851
5. Huang YJ, Hoffmann G, Wheeler B, Schiapparelli P, Quinones-Hinojosa A, Searson P. Cellular micro-environment modulates the galvanotaxis of brain tumor initiating cells. *Scientific Reports.* 2016; 6:21583. <https://doi.org/10.1038/srep21583>
6. Cooper MS, Keller RE. Perpendicular orientation and directional migration of amphibian neural crest cells in dc electrical fields. *Proceedings of the National Academy of Sciences of the United States of America.* 1984; 81(1):160–164. <https://doi.org/10.1073/pnas.81.1.160>
7. Sheridan DM, Isseroff RR, Nuccitelli R. Imposition of a Physiologic DC Electric Field Alters the Migratory Response of Human Keratinocytes on Extracellular Matrix Molecules. *Journal of Investigative Dermatology.* 1996; 106(4):642–646. <https://doi.org/10.1111/1523-1747.ep12345456>
8. Allen G, Mogilner A, Theriot J. Electrophoresis of Cellular Membrane Components Creates the Directional Cue Guiding Keratocyte Galvanotaxis. *Current Biology.* 2013; 23(7):560–568. <https://doi.org/10.1016/j.cub.2013.02.047>
9. Zhao M, McCaig CD, Agius-Fernandez A, Forrester JV, Araki-Sasaki K. Human corneal epithelial cells reorient and migrate cathodally in a small applied electric field. *Current Eye Research.* 1997; 16(10):973–984. <https://doi.org/10.1076/ceyr.16.10.973.9014>
10. Li X, Kolega J. Effects of Direct Current Electric Fields on Cell Migration and Actin Filament Distribution in Bovine Vascular Endothelial Cells. *Journal of Vascular Research.* 2002; 39(5):391–404. <https://doi.org/10.1159/000064517>
11. Rapp B, de Boisfleury-Chevance A, Gruler H. Galvanotaxis of human granulocytes. *European Biophysics Journal.* 1988; 16(5):313–319. <https://doi.org/10.1007/BF00254068>
12. Lin F, Baldessari F, Gyenge CC, Sato T, Chambers RD, Santiago JG, et al. Lymphocyte Electrotaxis In Vitro and In Vivo. *The Journal of Immunology.* 2008; 181(4):2465–2471. <https://doi.org/10.4049/jimmunol.181.4.2465> PMID: 18684937
13. L F Jaffe RN. Electrical Controls of Development. *Annual Review of Biophysics and Bioengineering.* 1977; 6(1):445–476. <https://doi.org/10.1146/annurev.bb.06.060177.002305>
14. Erickson C, Nuccitelli R. Embryonic fibroblast motility and orientation can be influenced by physiological electric fields. *The Journal of Cell Biology.* 1984; 98(1):296–307. <https://doi.org/10.1083/jcb.98.1.296>

15. Robinson KR. The responses of cells to electrical fields: a review. *The Journal of Cell Biology*. 1985; 101(6):2023–2027. <https://doi.org/10.1083/jcb.101.6.2023>
16. McCaig CD, Rajnicek AM, Song B, Zhao M. Controlling Cell Behavior Electrically: Current Views and Future Potential. *Physiological Reviews*. 2005; 85(3):943–978. <https://doi.org/10.1152/physrev.00020.2004>
17. McCaig CD, Song B, Rajnicek AM. Electrical dimensions in cell science. *Journal of Cell Science*. 2009; 122(23):4267–4276. <https://doi.org/10.1242/jcs.023564>
18. Mycielska ME, Djamgoz MBA. Cellular mechanisms of direct-current electric field effects: galvanotaxis and metastatic disease. *Journal of Cell Science*. 2004; 117(9):1631–1639. <https://doi.org/10.1242/jcs.01125>
19. Van Haastert PJM, Devreotes PN. Chemotaxis: signalling the way forward. *Nat Rev Mol Cell Biol*. 2004; 5(8):626–634. <https://doi.org/10.1038/nrm1435>
20. Zhao M, Jin T, McCaig CD, Forrester JV, Devreotes PN. Genetic analysis of the role of G protein-coupled receptor signaling in electrotaxis. *The Journal of cell biology*. 2002; 157(6):921–927. <https://doi.org/10.1083/jcb.200112070>
21. Zhao M, Song B, Pu J, Wada T, Reid B, Tai G, et al. Electrical signals control wound healing through phosphatidylinositol-3-OH kinase-gamma and PTEN. *Nature*. 2006; 442(7101):457–460. <https://doi.org/10.1038/nature04925> PMID: 16871217
22. Sato MJ, Ueda M, Takagi H, Watanabe TM, Yanagida T, Ueda M. Input-output relationship in galvanotactic response of Dictyostelium cells. *BioSystems*. 2007; 88(3):261–272. <https://doi.org/10.1016/j.biosystems.2006.06.008>
23. Sato MJ, Kuwayama H, van Egmond WN, Takayama ALK, Takagi H, van Haastert PJM, et al. Switching direction in electric-signal-induced cell migration by cyclic guanosine monophosphate and phosphatidylinositol signaling. *Proceedings of the National Academy of Sciences of the United States of America*. 2009; 106(16):6667–72. <https://doi.org/10.1073/pnas.0809974106> PMID: 19346484
24. Gao R, Zhao S, Jiang X, Sun Y, Zhao S, Gao J, et al. A large-scale screen reveals genes that mediate electrotaxis in Dictyostelium discoideum. *Science Signaling*. 2015; 8(378):ra50. <https://doi.org/10.1126/scisignal.aab0562> PMID: 26012633
25. Yuen IS, Jain R, Bishop JD, Lindsey DF, Deery WJ, Van Haastert PJ, et al. A density-sensing factor regulates signal transduction in Dictyostelium. *The Journal of Cell Biology*. 1995; 129(5):1251–1262. <https://doi.org/10.1083/jcb.129.5.1251> PMID: 7775572
26. Clarke M, Gomer RH. PSF and CMF, autocrine factors that regulate gene expression during growth and early development of Dictyostelium. *Experientia*. 1995; 51(12):1124–1134. <https://doi.org/10.1007/BF01944730>
27. Gomer RH, Jang W, Brazill D. Cell density sensing and size determination. *Development, growth & differentiation*. 2011; 53(4):482–494. <https://doi.org/10.1111/j.1440-169X.2010.01248.x>
28. Amselem G, Theves M, Bae A, Bodenschatz E, Beta C. A Stochastic Description of Dictyostelium Chemotaxis. *PLOS ONE*. 2012; 7(5):1–11.
29. Gao R, Zhang X, Sun Y, Kamimura Y, Mogilner A, Devreotes PN, et al. Different Roles of Membrane Potentials in Electrotaxis and Chemotaxis of Dictyostelium Cells. *Eukaryotic Cell*. 2011; 10(9):1251–1256. <https://doi.org/10.1128/EC.05066-11> PMID: 21743003
30. Beta C, Frohlich T, Bodeker HU, Bodenschatz E. Chemotaxis in microfluidic devices—a study of flow effects. *Lab Chip*. 2008; 8:1087–1096. <https://doi.org/10.1039/b801331d>
31. Décavé E, Garrivier D, Bréchet Y, Fourcade B, Bruckert F. Shear flow-induced detachment kinetics of Dictyostelium discoideum cells from solid substrate. *Biophysical journal*. 2002; 82(5):2383–2395. [https://doi.org/10.1016/S0006-3495\(02\)75583-5](https://doi.org/10.1016/S0006-3495(02)75583-5)
32. Décavé E, Rieu D, Dalous J, Fache S, Brechet Y, Fourcade B, et al. Shear flow-induced motility of Dictyostelium discoideum cells on solid substrate. *Journal of Cell Science*. 2003; 116(Pt 21):4331–4343. PMID: 12966168
33. Shanley LJ, Walczysko P, Bain M, MacEwan DJ, Zhao M. Influx of extracellular Ca²⁺ is necessary for electrotaxis in Dictyostelium. *Journal of Cell Science*. 2006; 119(22):4741–4748. <https://doi.org/10.1242/jcs.03248>
34. Van Haastert PJM, Devreotes PN. Chemotaxis: signalling the way forward. *Nat Rev Mol Cell Biol*. 2004; 5(8):626–634. <https://doi.org/10.1038/nrm1435>
35. Gomer RH, Yuen IS, Firtel RA. A secreted 80 × 10(3) Mr protein mediates sensing of cell density and the onset of development in Dictyostelium. *Development*. 1991; 112(1):269–278.
36. Yuen IS, Taphouse C, Halfant KA, Gomer RH. Regulation and processing of a secreted protein that mediates sensing of cell density in Dictyostelium. *Development*. 1991; 113(4):1375–1385.

37. Jain R, Gomer RH. A developmentally regulated cell surface receptor for a density-sensing factor in Dictyostelium. *Journal of Biological Chemistry*. 1994; 269(12):9128–9136.
38. Zouwail S, Pettitt TR, Dove SK, Chibalina MV, Powner DJ, Haynes L, et al. Phospholipase D activity is essential for actin localization and actin-based motility in Dictyostelium. *Biochemical Journal*. 2005; 389 (Pt 1):207–214. <https://doi.org/10.1042/BJ20050085> PMID: 15769249